DIGITAL SIGNAL ANALYSIS OF METAL ELECTROREDUCTION CELLS

RANA P. SINGH
JOHN H. FLINT
DONALD R. SADOWAY

DEPARTMENT OF MATERIALS SCIENCE AND ENGINEERING
MASSACHUSETTS INSTITUTE OF TECHNOLOGY
CAMBRIDGE, MASSACHUSETTS

ABSTRACT

Electrolytic metal reduction operatios in both aqueous and molten salt electrolytes are being studied by digital signal analysis. The purpose is to determine the relationship between the physical processes occurring in the cell and the frequency spectrum of the cell's fluctuating electrical parameters. The fast Fourier transform of cell voltage (in galvanostatic operations) or cell current (in potentiostatic operations) is computed on-line in real time for the electrorefining of zinc in aqueous acid chloride solutions.

INTRODUCTION

Industrial electrodeposition processes are complex operations which must be controlled to achieve desired efficiency and to maintain product quality. Furthermore, because the deposition cycles are very long, several days to several weeks, it is desirable to have on-line continuous monitoring, to minimize the deleterious effects of changes in operating conditions over such extended time periods.

Digital signal processing is a rapidly growing field which has touched such diverse areas as telecommunications (Freeny, Kaiser and McDonald, 1978), audio recording/playback (Blesser and Kates, 1978), and visual image enhancement (Hunt, 1978). The purpose of the present study is to determine whether digital signal analysis by fast Fourier transform of the electrical characteristics of an operating electrolytic cell can serve as the basis of diagnostic instrumentation for control and automation of electrolytic processes. Two systems are under study: the electrorefining of zinc in aqueous acid chloride solutions and the electrodeposition of manganese in alkali chloride melts. The results of aqueous zinc studies are presented here.

When a metal electroreduction cell is operating, the measured cell voltage, E_{cell}, can be divided into the following components (Stender, Zivotinsky, and Stroganoff, 1934):

$$E_{cell} = E_{rev} + E_{ohm} + E_{contact} + \eta_{cathode} + \eta_{anode} \quad [1]$$

where E_{rev} is the reversible cell potential, E_{ohm} is the ohmic drop across the electrolyte and may include the iR drop of the electrolyte itself and a contribution from gas bubbles at the electrodes, $E_{contact}$ is the contact resistance at the points where the conductors from the power supply are connected to the electrodes, and η is the overvoltage at the specified electrode. Depending upon the cell design and operating conditions, the magnitude of each term will vary. For example, during gas evolution at the anode in an electrowinning operation bubbles of chlorine displace the electrolyte from the electrode (Piontelli et al., 1965). The electrical impedance of the cell rises until the bubble detaches. The electrolyte then flows back to make electrical contact with the electrode again, and the cell impedance drops. If such a cell were being driven galvanostatically, the rise and fall of cell impedance would be reflected in the cell voltage (Tunold et al., 1971). This fluctuation in cell voltage due to gas evolution is expected to have its own characteristic electrical signature, which is difficult to identify when seen against a background of normal voltage fluctuations on a plot of voltage versus time. However, by digital signal processing it is possible to suppress random fluctuations and through spectrum analysis reveal the electrical signals associated with physical processes occurring in the cell. In other words, by the use of fast Fourier transform, periodic phenomena which cannot be observed in time domain can be elucidated in frequency domain.

The general applications of digital signal processing and the mathematics of discrete Fourier transform are reported in the literature (Beauchamp and Yuen, 1979; Otnes and Enochson, 1972; Searns, 1983). The fast Fourier transform technique has been used for studying electrode kinetics (Pilla, 1970; Creason and Smith, 1972; Ichise et al., 1971). There are no reports of any real-time application of digital signal processing using the fast Fourier transform technique on metal reduction cells during operation.

EXPERIMENTAL

In order to test whether the frequency spectrum of the electrical characteristics of the electrolysis cell was representative of the physical processes occuring in the cell, the cell's operating conditions were varied and the electrical response was observed. Specifically, the electrode arrangement and the applied overpotential were varied. Finally, the effect of an organic additive was studied.

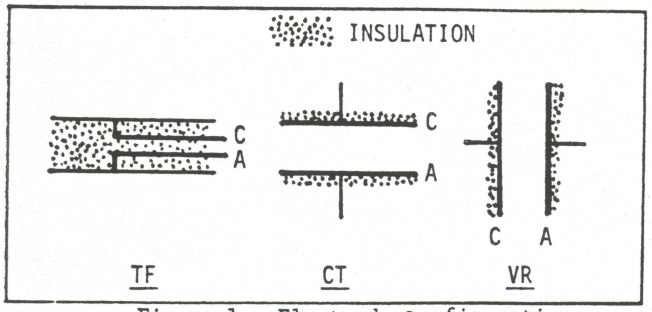

Figure 1. Electrode configurations

Figure 1 shows the three electrode configurations that were studied. In the TF (top free) arrangement the anode is placed below the cathode and is facing downward so that as the anode dissolves, the electrolyte circulation pattern near the cathode is not affected. In the CT (cathode on top) arrangement, cathodic deposition renders the electrolyte next to the cathode less dense than the bulk electrolyte and produces an entirely different electrolyte circulation pattern from TF. Furthermore, at high values of applied overpotential, hydrogen bubbles evolve on the cathode to produce a sort of "cathode effect" analogous to the anode effect observed in the molten salt electrolysis of aluminum. The VR arrangement consists simply of parallel-plate vertical electrodes. In all arrangements the electrodes are electrically insulated so that only the "front" surface is active.

The electrochemical cell was a 2" glass cube. Electrode holders were machined out of polymethyl methacrylate. Both the anode and the cathode were pure zinc (99.99%) discs, 1" in diameter and 10 mils (0.25 mm) thick, with an active surface area of 5.07 cm^2. First they were polished mechanically using 600 grit emery paper. They were then dipped into a 50% HCl solution for several seconds, rinsed, installed wet on the electrode holder and immersed in the electrolyte as soon as possible. The composition of the electrolyte was fixed at 0.3 M $ZnCl_2$, 3 M NaCl, pH = 2.5. Salts were of analytical grade. The pH was adjusted by additions of hydrochloric acid. In a separate vessel containing the identical electrolyte, a standard calomel electrode served as a reference. Contact with the electrochemical cell was made through tubing at the end of which was a Luggin capillary positioned at a distance of less than 1 mm from the cathode surface. The potentiostat was an Aardvark, Model V-2. A power booster, Aardvark Model X, raised the maximum current capacity of the potentiostat to 10 A.

Electrolysis was conducted potentiostatically. Applied overpotential was set at three values: one where the induction time for dendrite growth is long in comparison with the duration of the experiment and the other two where codeposition of hydrogen with zinc is evident. These values had been measured previously in this laboratory (Abdelmassih and Sadoway, 1983). Fluctuations in current at constant voltage were monitored at frequencies spanning the interval 10^{-2} to 10 Hz, which had been previously determined by signal analysis to discover which frequencies were present. The cell current output was connected through a low-pass filter set at 10 Hz to the A/D converter of the computer (Digital Equipment Corp, MINC 11/23). The sampling rate was 20 Hz. The computer was programmed to sample the signal for 50 seconds, perform the fast Fourier transform, and plot the results while continuing to take data for the next sampling period. This was done on-line in real time.

RESULTS AND DISCUSSION

Figures 2, 3 and 4 show the frequency spectra taken at 60mV, 170mV, and 700 mV respectively, with horizontal electrodes, TF configuration. Each figure displays the amplitude of the current as a function of frequency. The results of each successive 50-second sampling period are offset upwards for ease of viewing. Figure 2 shows that at 60 mV, which is below the critical overpotential for dendrite growth, there is very little activity in the frequency spectrum. The average current was 25 mA and remained virtually unchanged for the duration of the experiment. Figure 3 shows that at 170 mV, which is above the critical overpotential for dendrite growth, there is evidence of activity centered about 0.02 Hz. Figure 4 shows that at 700 mV the frequency spectrum is very active, particularly from 0.05 - 0.3 Hz. Superimposed on this is the tendency for the spectrum to ramp up at low frequencies. Vigorous hydrogen bubbling which was plainly visible is thought to cause the roughness of the spectrum, while the low frequency ramp is thought to be caused by surface roughening of the cathode deposit. This will be explained later.

Figures 5, 6 and 7 show the frequency spectra taken at 60 mV, 170 mV and 700 mV, respectively, with vertical electrodes. At low and intermediate overpotentials, the spectra are smoother than those taken with the TF configuration. This can be explained by the enhanced mass transfer to vertical electrodes as a result of density-driven convection. At the highest overpotential, 700 mV, the hydrogen bubbling appears to be more disruptive at vertical electrodes than at horizontal electrodes. The steady-state average current for TF was 220 - 400 mA, and for VR it was 400 - 600 mA. Note that Figure 7 has twice the scale factor of the previous figures.

Figures 8 and 9 show the frequency spectra taken at 60 mV and 500 mV, respectively, with horizontal electrodes, CT configuration. At the low overpotential, the spectrum is as smooth as the 60 mV spectrum at vertical electrodes, but shows a much more pronounced low frequency rise. At 500 mV the spectrum is rougher than at 60 mV, but the low frequency rise is absent. With the cathode facing down at the top of the cell, there is little to drive convection. As the electrolyte next to the cathode is depleted of zinc it becomes less dense than the bulk. Mass transfer is diffusion-controlled. Surface roughening occurs. Vigorous hydrogen bubbling can be viewed as beneficial to this electrode configuration, as it agitates the electrolyte and improves circulation.

It appears that low frequency rise in the power spectrum can be explained by surface roughening of the cathodic deposit. Figure 10 shows a sinusoidal wave form (f = 0.2 Hz) superimposed on a ramp. Figure 11 is the Fourier transform. The spike at 0.2

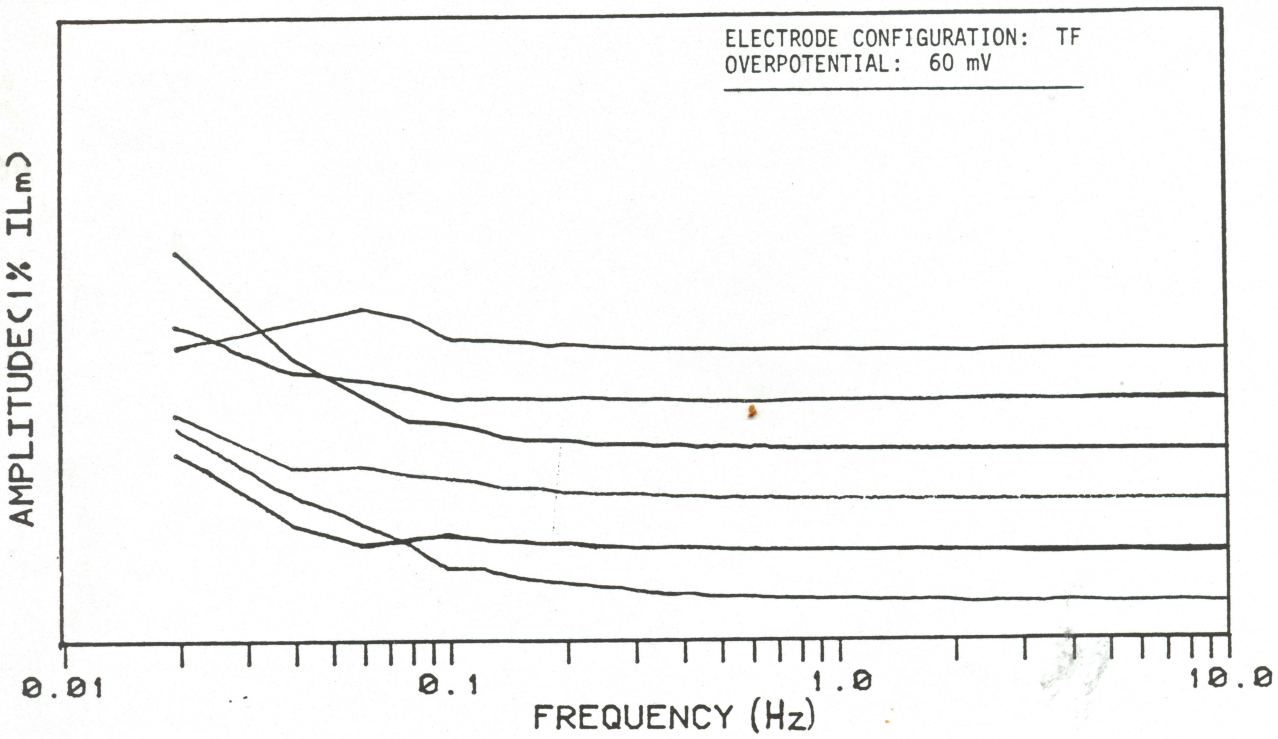

Figure 2. Frequency spectrum of cell current.

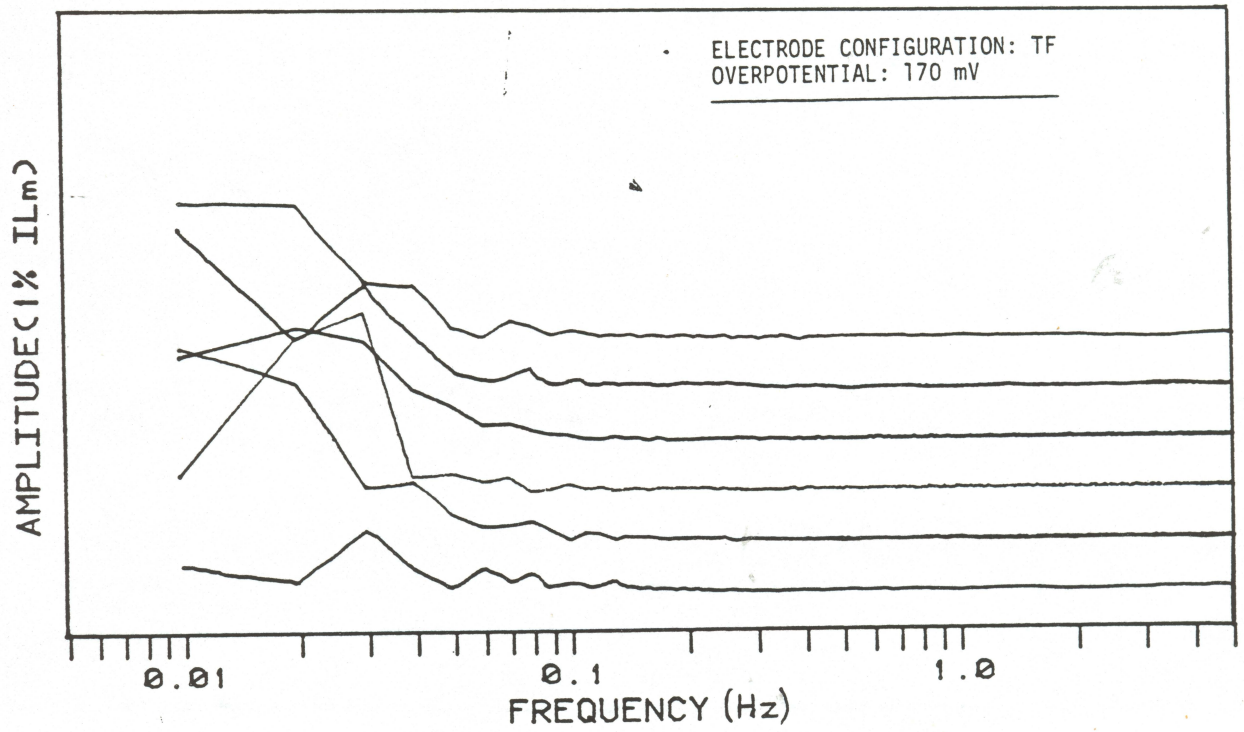

Figure 3. Frequency spectrum of cell current.

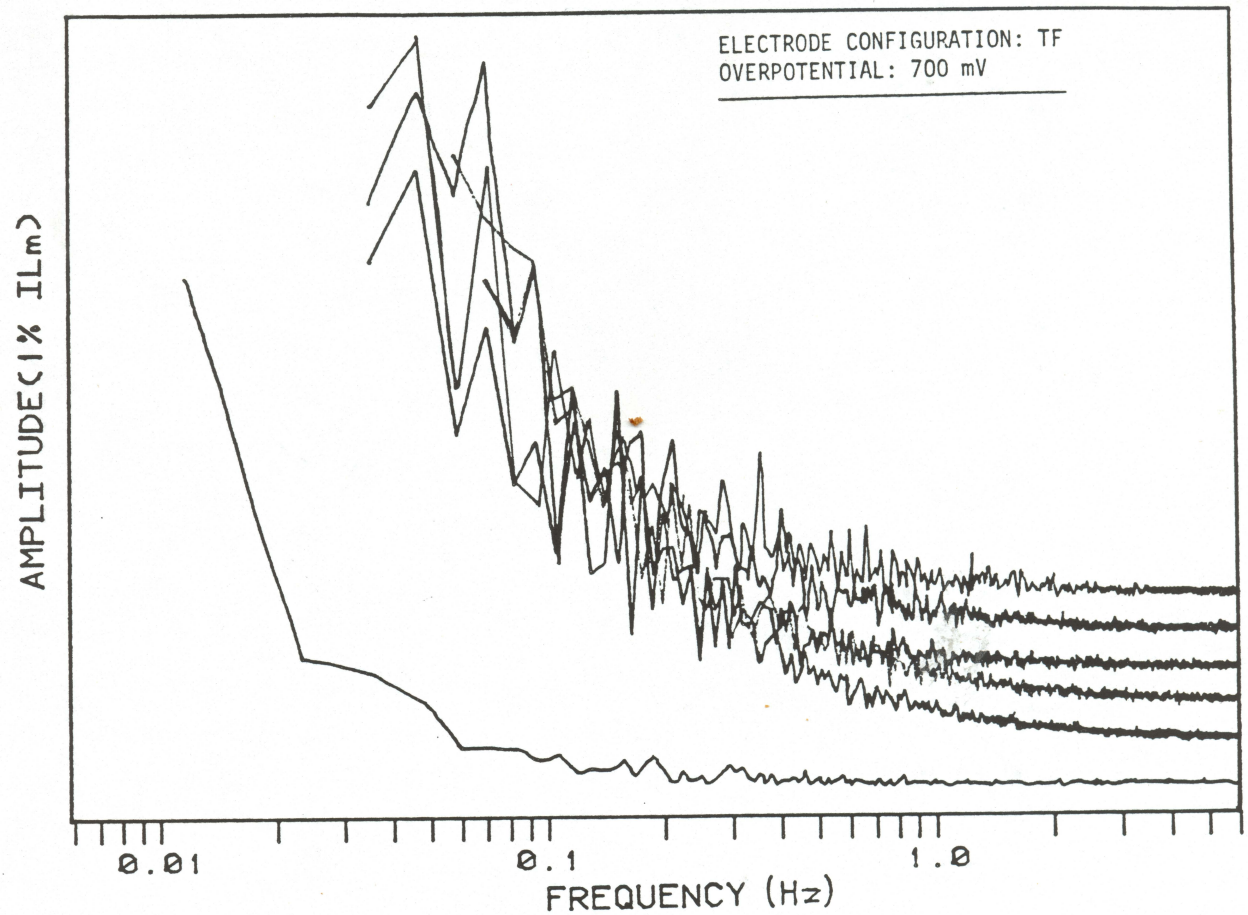

Figure 4. Frequency spectrum of cell current.

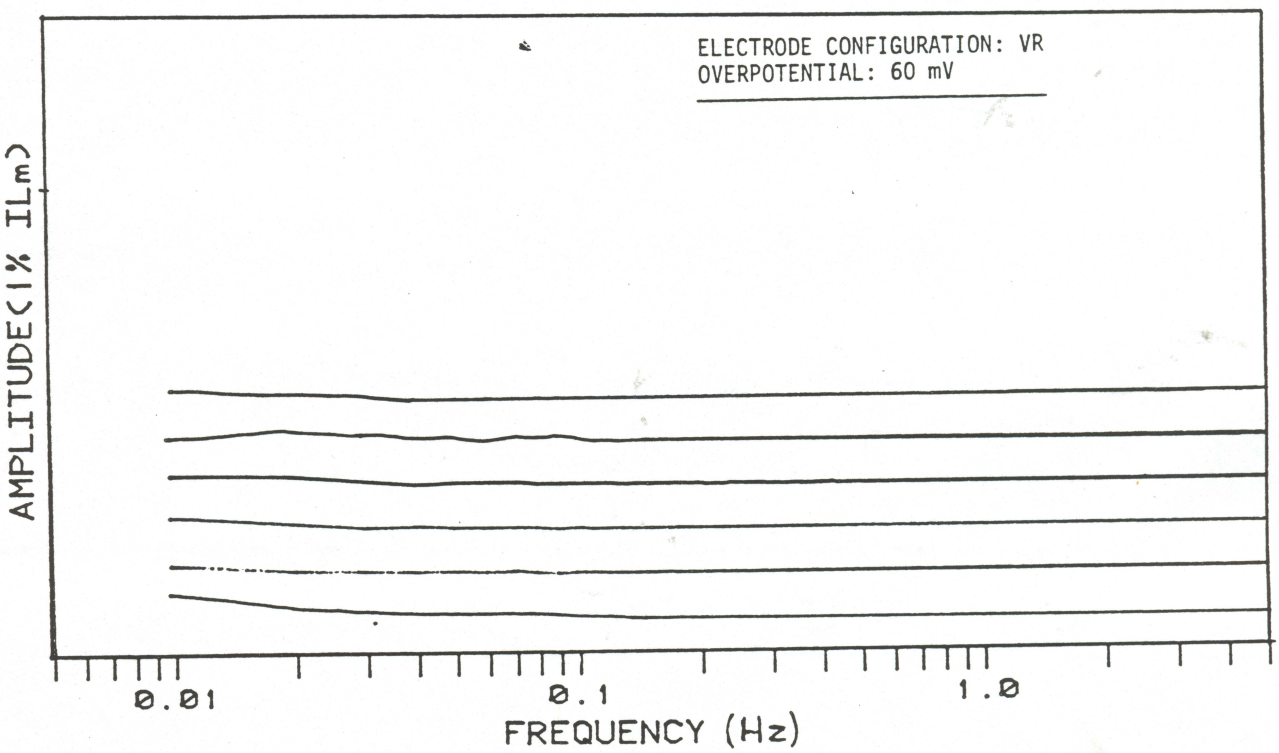

Figure 5. Frequency spectrum of cell current.

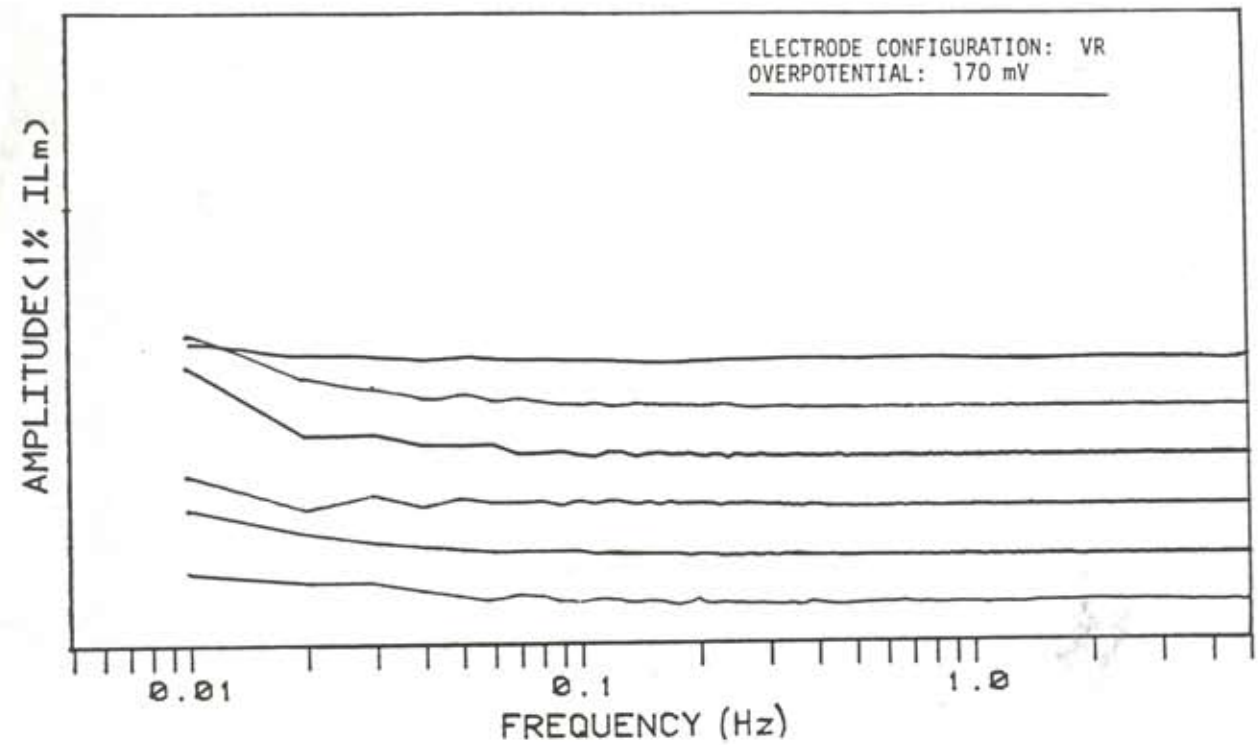

Figure 6. Frequency spectrum of cell current.

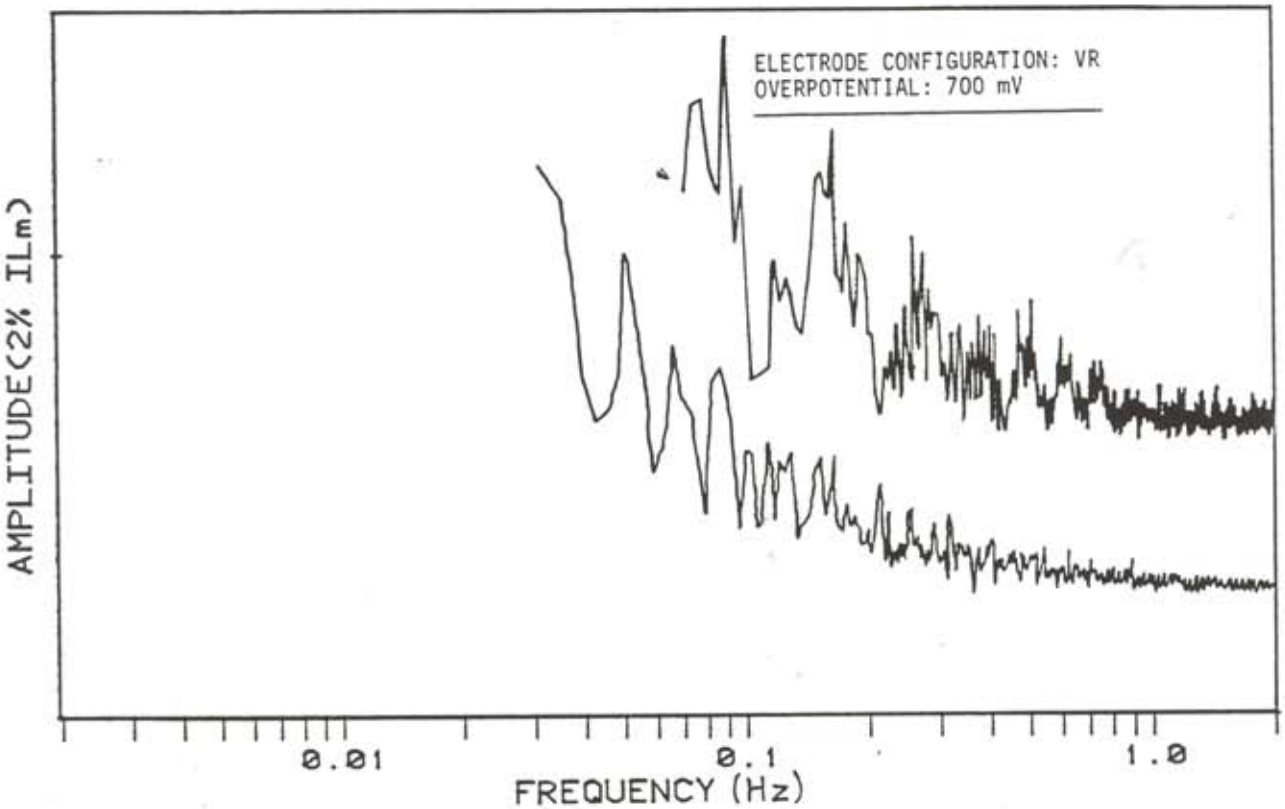

Figure 7. Frequency spectrum of cell current.

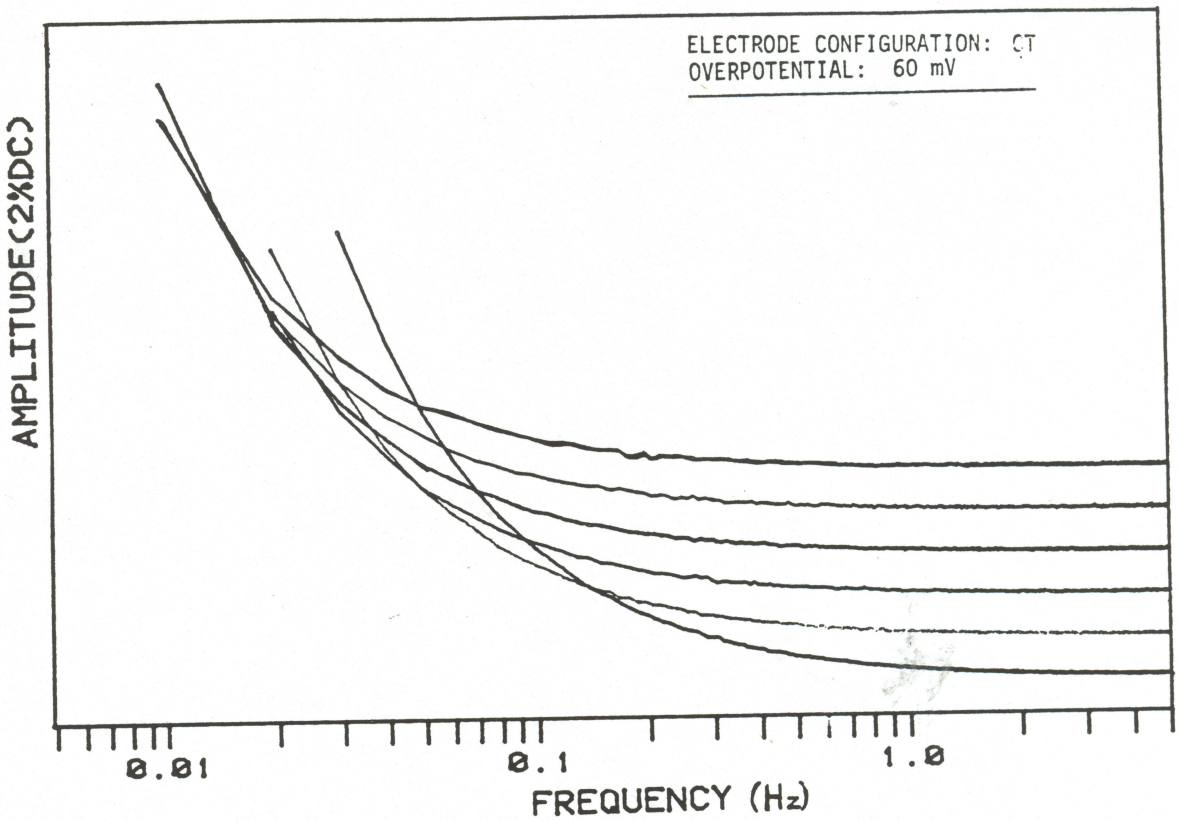

Figure 8. Frequency spectrum of cell current.

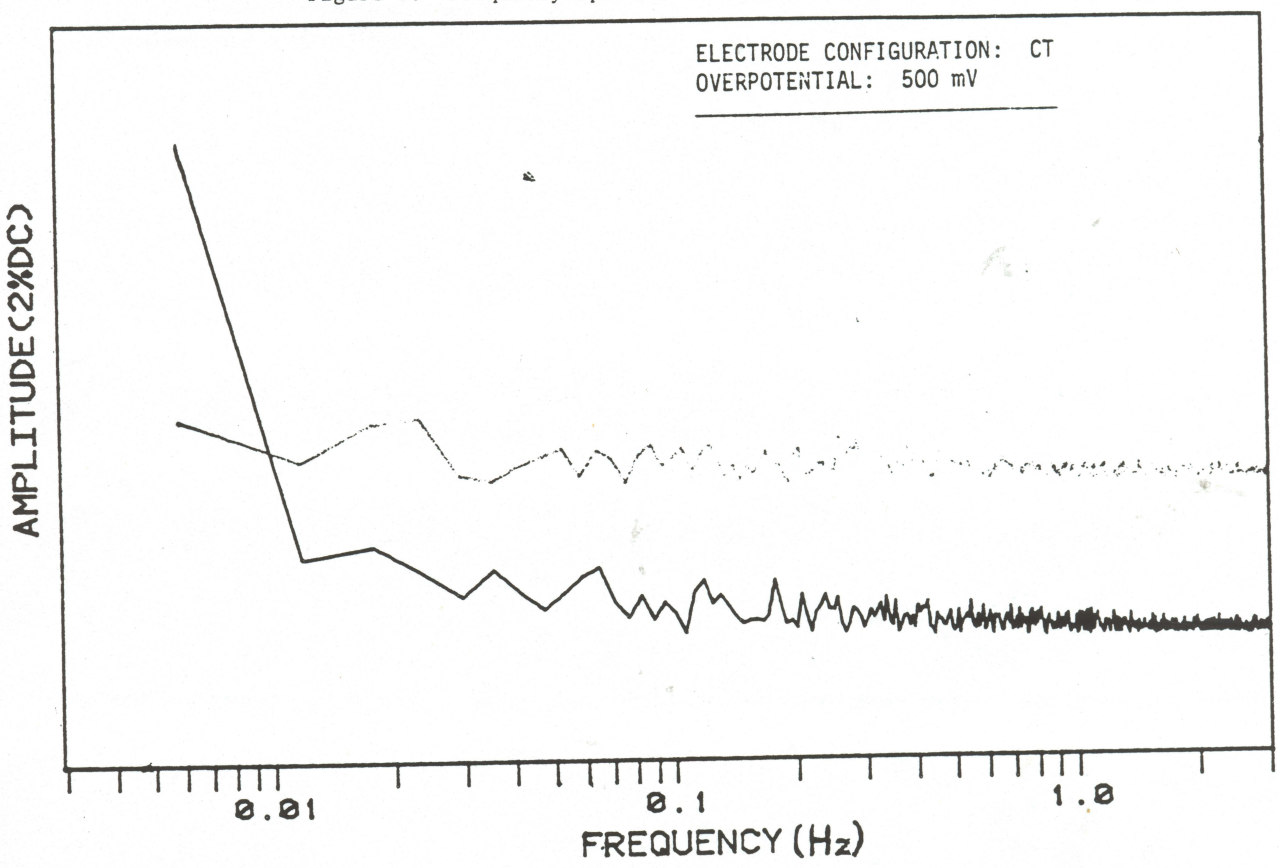

Figure 9. Frequency spectrum of cell current.

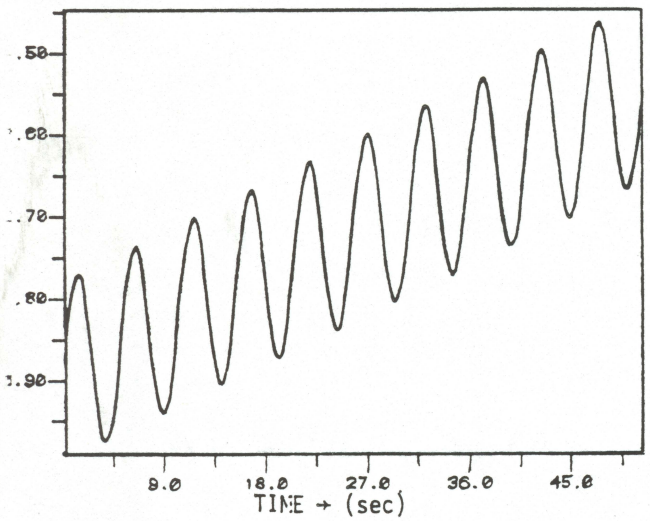

Figure 10. Computer-generated waveform: 0.2 Hz sine wave superimposed on a ramp.

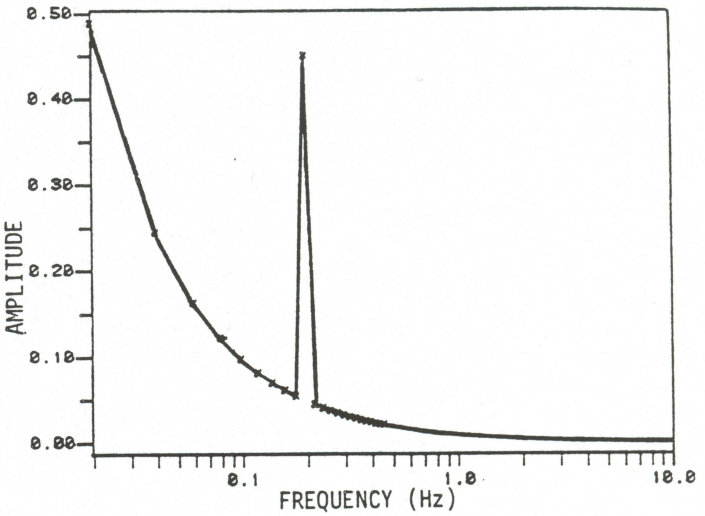

Figure 11. Frequency spectrum of waveform in Figure 10.

is due to the periodicity of the fluctuation and e low frequency rise is due to the ramp. During ectrodeposition at constant voltage, an increase surface area would be accompanied by an increase current. In fact, such an increase in average ll current was observed in the experiments report- here. It is too early to state that only surface ughening can cause the low frequency rise, but itial results seem to indicate that it is the imary cause.

The effect of organic additives was studied by peating some of the earlier electrodeposition experiments with the addition of glucose. Figure 12 shows the frequency spectrum of the fluctuating cell current for a TF electrode configuration and an applied overpotential of 170 mV. Figure 3 shows the results for the identical experiment performed without glucose in the electrolyte. Both figures are drawn to the same scale. The spectrum of Figure 12 lacks the low frequency peaks of Figure 3.

Figures 13 and 14 are SEM photographs showing surface detail of the deposits associated with Figures 3 and 12, respectively. Figure 13 shows evidence of faceting, while in Figure 14 it appears

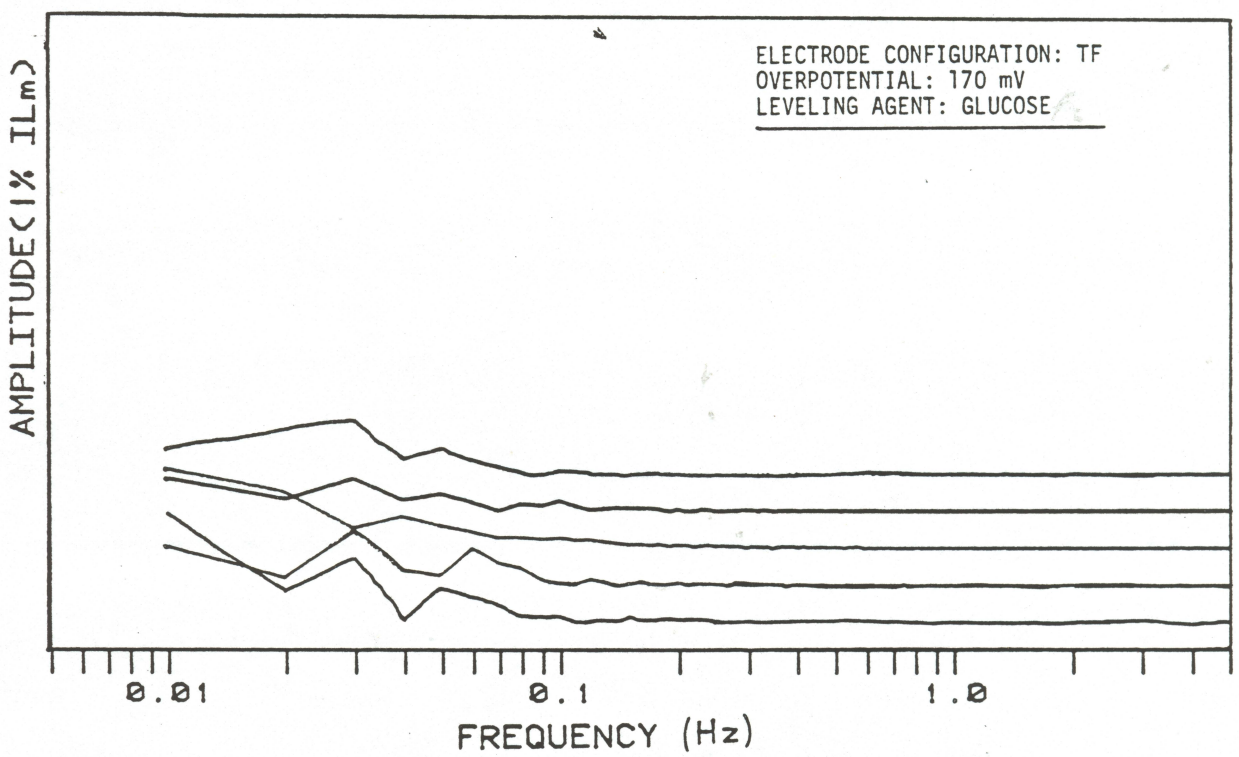

Figure 12. Frequency spectrum of cell current.

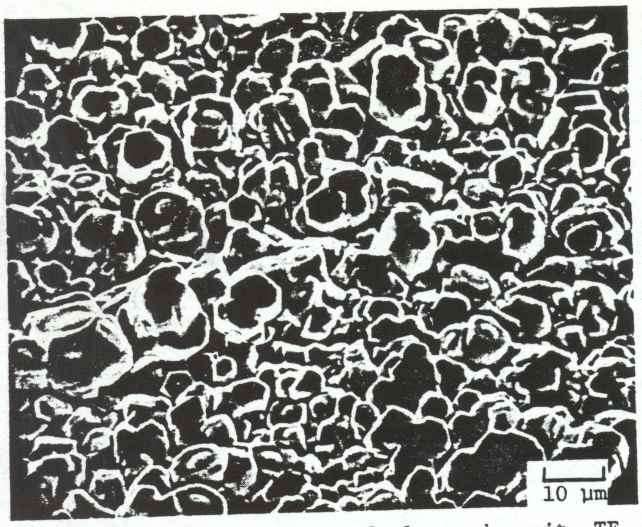

Figure 13. SEM photograph of electrodeposit. TF configuration. η = 170 mV. Stock electrolyte.

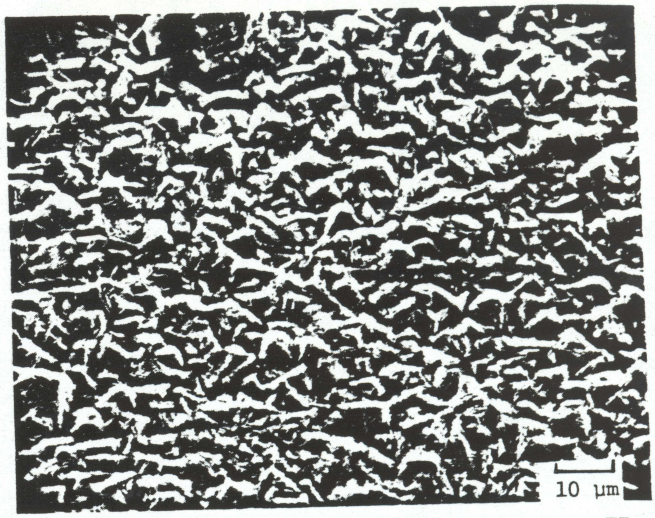

Figure 14. SEM photograph of electrodeposit. TF configuration. η = 170 mV. Glucose added to stock electrolyte.

that the glucose has suppressed this tendency. Perhaps the low frequency peaks in Fig. 3 are the electrical signature of the faceting seen in Fig. 13. If so, then by digital signal analysis it should be possible to sense when the electrolyte has been depleted of levelling agent by comparing the real time spectra taken on-line to a reference spectrum. When the difference in the two spectra exceeds an experimentally determined tolerance limit over the previously noted low frequency interval, more levelling agent should be added. One of the attractive features of such a control technique is that it could be retrofitted to existing cells.

SUMMARY

On the basis of this initial study of the electrorefining of zinc in acid chloride electrolytes, it is concluded that different physical conditions in the electrolysis operation give different frequency spectra. However, at this time it is not possible to define unambiguously the electrical signature of each physical process. It does appear that surface roughness is associated with low frequency rise in the frequency spectrum of the fluctuating cell current. Similar experiments are now being conducted on the fused salt electrolysis of manganese from $MnCl_2$-alkali chloride melts.

ACKNOWLEDGEMENT

The authors gratefully acknowledge the financial support of the National Science Foundation through Grant No. CPE-8116641.

REFERENCES

Abdelmassih, A., and Sadoway, D. R., 1983, "Laser Schlieren Studies of Aqueous Zinc Chloride Electrolysis," Chloride Electrometallurgy, Parker, P.D., ed., TMS-AIME, Warrendale, PA, pp. 43-57.

Beauchamp, K. G., and Yuen, C. K., 1979, Digital Methods for Signal Analysis, John Wiley and Sons, Inc., New York.

Blesser, B., and Kates, J. M., 1978, "Digital Processing in Audio Signals," Applications of Digital Signal Processing, Oppenhiem, A.V., ed., Prentice-Hall, Englewood Cliffs, N. J.

Creason, S.C., and Smith, D.E., 1972, "Fourier Transform Faradaic Admittance Measurements. I. Demonstration of the Applicability of Random and Pseudorandom Noise as Applied Potential Signals," Journal of Electroanalytical Chemistry and Interfacial Electrochemistry, Volume 36, pp. 1111-1117.

Freeny, S.L., Kaiser, J.F., and McDonald, H.S., 1978, "Some Applications of Digital Signal Processing in Telecommunications," Applications of Digital Signal Processing, Oppenheim, A.V., ed., Prentice-Hall, Englewood Cliffs, N.J.

Hunt, B.R., 1978, "Digital Image Processing," ibid.

Ichise, M., Nagayanagi, Y., and Kojima, T., 1971, "Analog Simulation of Noninteger Order Transfer Function for Analysis of Electrode Processes," Journal of Electroanalytical Chemistry and Interfacial Electrochemistry, Volume 33, pp. 253-265.

Otnes, R.K., and Enochson, L., 1972, Digital Time Series Analysis, John Wiley and Sons, Inc. N. Y.

Pilla, A.A., 1970, "Transient Impedance Technique for the Study of Electrode Kinetics. Application to Potentiostatic Methods," Journal of the Electrochemical Society, Volume 117, pp. 467-477.

Piontelli, R., et al., 1966, "Cinematographic Study of the Anodic Chlorine Development from Molten Salts and Aqueous Solutions," (in Italian), Electrochemica Metallorum, Volume 1, pp. 279-294.

Searns, S.D., 1983, Digital Signal Analysis, Hayden Book Co, Inc., Rochelle Park, N. J.

Stender, V.V., Zivotinsky, P.B., and Stroganoff, M.M., 1934, "The Voltage Balance of a Cell for the Electrolysis of Sodium Chloride Solutions," Transactions of the Electrochemical Society, Volume 65, pp. 189-212.

Tunold, R., et al., 1971, "Chlorine Evolution on Graphite Anodes in a NaCl-AgCl Melt," Electrochimica Acta, Volume 16, pp. 2101-2120.